Journal Pre-proof

Adherens junctions are involved in polarized contractile ring formation in dividing epithelial cells of *Xenopus laevis* embryos

Guillaume Hatte[1], Claude Prigent[1,2] and Jean-Pierre Tassan[1]*

1 : Univ Rennes, CNRS, IGDR (Institut de Génétique et Développement de Rennes), UMR 6290, 2 Avenue du Professeur Leon Bernard, 35000 Rennes, France

2 : Present address starting January 1st, 2021 : Centre de Recherche de Biologie cellulaire de Montpellier (CRBM), University of Montpellier, CNRS, 34293 Montpellier, France.

* Corresponding author.

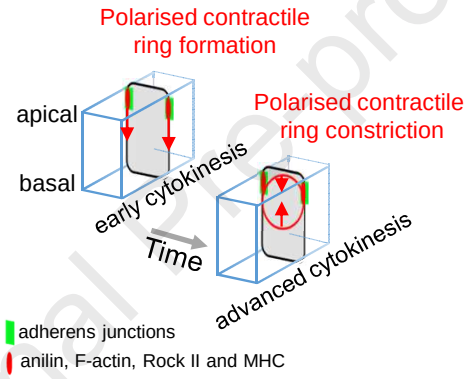
E-mail address : jean-pierre.tassan@univ-rennes1.fr

Journal Pre-proof

Author contributions

G.H. carried out the experiments, generated and interpreted the data. J-P.T. designed research and supervised the project. G.H., C.P. and J-P. T. wrote the manuscript.

Journal Pre-proof



Journal Pre-proof

Journal Pre-proof

Abstract

Cells dividing in the plane of epithelial tissues proceed by polarized constriction of the actomyosin contractile ring, leading to asymmetric ingression of the plasma mem brane. Asymmetric cytokinesis results in the apical positioning of the actomyosin contractile ring and ultimately of the midbody. Studies have indicated that the contractile ring is associated with adherens junctions, whose role is to maintain epithelial tissue cohesion. However, it is yet unknown when the contractile ring becomes associated with adherens junctions in epithelial cells. Here, we examined contractile ring formation and activation in the epithelium of *Xenopus* embryos and explored the implication of adherens junctions in the contractile ring formation. We show that accumulation of proteins involved in contractile ring formation and activation is polarized, starting at apical cell-cell contacts at the presumptive division site and spreading within seconds towards the cell basal side. We also show that adherens junctions are involved in the kinetics of contractile ring formation. Our study reveals that the link between the adherens junctions and the contractile ring is established from the onset of cytokinesis.

Keywords: cytokinesis, actomyosin, asymmetric furrowing, cell division, polarity

Journal Pre-proof

1. Introduction

Mitotic cells divide to produce two daughter cells in a process called cytokinesis, which relies upon contraction of an actomyosin ring placed at the cell equator. The contractile ring is constituted of actin filaments and the non-muscular motor protein myosin II [1]. In isolated cells, the actomyosin ring contracts symmetrically, ingressing the cell plasma membrane all around the mother cell midzone in an isoconcentric manner. The contractile actomyosin ring must be accurately positioned at the equatorial cortex to bisect the mitotic spindle and equally distribute the chromosomes. This appropriate positioning is ensured by signals emanating from the mitotic spindle in late anaphase. The building and contraction of the contractile actomyosin ring requires activation of the small regulatory GTPase RhoA by the GTPase Exchange Factor (GEF) Ect2. Centralspindlin, a heterotetramer of the kinesin-related protein MLKP1 and the GTPase-activating protein (GAP) MgcRacGAP, which interacts with microtubules of the central spindle, delivers Ect2 to the cell cortex, where it activates RhoA. Activated RhoA regulates simultaneously the polymerization of actin filaments (F-actin) and activation of non-muscular myosin II, thereby leading to constriction of the cytokinetic ring [1]. These regulations by RhoA happen *via* concomitant activation of formins which increases actin polymerisation and activation of the Rho-associated coiled-coil containing protein kinase II (Rock II). Rock II in turn phosphorylates myosin light chain, thus activating myosin. In addition to actin and myosin II, other proteins are components of the contractile ring, including the scaffolding protein anillin which anchors the contractile ring to the cell plasma membrane, maintains the furrow stability and is necessary for effective RhoA-mediated contractility [2–5].

In contrast to the isoconcentric furrowing that occurs when isolated cells divide, contraction of the actomyosin ring is polarized in cells dividing in the plane of an epithelium, likely reflecting their marked apical-basolateral polarity. Furrowing typically progresses from the cell's basal side towards the apical surface. This mode of cytokinesis by asymmetric furrowing has been reported in diverse model systems, including insects and vertebrates, suggesting that asymmetric furrowing is the default mode of cytokinesis in epithelia [6,7]. Asymmetric furrowing is intimately linked to epithelial cell polarity. Epithelial cells have distinct apical and basolateral plasma membrane domains, separated by a belt of tight and adherens junctions [8–11].

Adherens junctions participate in the maintenance of epithelial tissue integrity. They are constituted of the transmembrane protein cadherin, which creates, *via* its extracellular domain, homophilic interactions with cadherin of neighbouring cells. Through interactions of its intracytoplasmic tail with α and β -catenins, cadherin is indirectly connected to the apical actomyosin belt, which maintains epithelial cell shape and epithelial integrity.

In *Drosophila*, it has been shown that adherens junctions contribute to the asymmetry of furrowing of dividing cells [12,13]. The cytokinetic ring constriction, which is normally asymmetric in Drosophila epithelial cells, becomes symmetric in cells depleted of β-catenin or E-cadherin. These studies demonstrate the importance of adherens junctions for asymmetric furrowing and anchoring of the contractile ring for apical positioning of the midbody. However, it remains largely unknown how the contractile ring forms and when it becomes connected to adherens junctions.

Here, we used the epithelium of *Xenopus laevis* embryos at the gastrula stage to study contractile ring formation, because at this developmental stage, cells divide exclusively parallel to the epithelium plane such that both daughter cells remain continuously in that plane [14]. Moreover, we have previously shown that epithelial cells divide by asymmetric furrowing from the basal towards the apical side [15]. Using live imaging of *Xenopus* laevis gastrula embryos expressing several contractile actomyosin ring components, we have here characterized the dynamics of contractile ring formation and have shown that the contractile ring formation is polarized from apical cell-cell junctions towards the cell basal side. Activation of the contractile motor protein myosin II leading to the contraction of the actomyosin ring is also polarized. Finally, we shown that adherens junctions are involved in the formation kinetics of the contractile ring.

2. Materials and Methods

2.1 Plasmids

Plasmids pCS2-Lifeact-GFP (a kind gift from Ulrike Engel, Heidelberg University, Germany), pCS2-mRFP-GPI, pCS2-GFP-GPI (a kind gift from Mikael Brand,

Dresden University of Technology, Germany), pCS2-GFP-rGBD (a kind gift from William Bement), pSp64T-C-cad Ctail [16], pT7T-ZO-1-GFP [17] and pT7T-SF9-GFP [18] were used in this study. pT7T-GFP-Rock II K/R was constructed by site-directed mutagenesis of lysine 117 (K117) from *Xenopus* Rock II (a kind gift from Johné Liu, [19]). The K117, essential for the catalytic activity of the kinase, was replaced by an arginine to abolish Rock II activity because the overexpression of the active kinase causes division defects, which are not obtained with the Rock II K/R mutant. The amplification product was cloned into the vector pT7T in phase with N-terminal GFP. PT7T-3xGFP-anillin was constructed by PCR amplification of the *Xenopus* anillin sequence, from the plasmid pT7T-GFP-Xlanillin [15] and subcloned into pT7T-3xGFP with N-terminal 3xGFP. All new constructs were verified by sequencing. All plasmids were linearised to generate mRNAs by *in vitro* transcription using the T7 or SP6 mMessage mMachine kit (Ambion).

2.2 α-catenin and ZO-1 knockdown

For α-catenin and ZO-1 knockdown experiments, antisense morpholinos targeting the initiation codon of respectively α-catenin (5′-ATGTTTCCTGTATTGAGAGTCATGC-3′) and ZO-1 (5′-GCCGGTGTCAGTATGAGTCCCCAGA-3′) were produced by Gene Tools. These morpholinos were previously characterized [17,20]. A standard morpholino (5′-CTCTTACCTCAGTTACAATTTATA-3′, Gene Tools) was used as a control.

2.3 Preparation of Xenopus laevis embryos and microinjection

Xenopus laevis albinos were obtained from Biological Resources Centre (CRB, Rennes, France). All animal experiments were performed in accordance with the approved protocols and guidelines at Rennes 1 University by the Comité Rennais d'Ethique en Matière d'Expérimentation Animale (C2EA-07) and the French Ministry for Education and Research (3523813). Eggs were fertilized *in vitro* and embryos were collected as described previously [18]. After de-jelling, embryos were placed in 5% Ficoll in F1 buffer (10 mM HEPES pH 7.6, 31.2 mM NaCl, 1.75 mM KCl, 59 µM MgCl2, 2 mM NaHCO3, and 0.25 mM CaCl2) for microinjection. mRNAs were

microinjected into one blastomere of 4- or 8-cell-stage embryos. For α-catenin knockdown experiments, 20 ng of α-catenin antisense morpholino in 9.2 nl was microinjected into one blastomere at the 8-cell stage. For α-catenin and ZO-1 double knockdown, respectively 20 ng and 40 ng of morphilonos were microinjected. Embryos were then placed at 16°C overnight and analyzed at the gastrula stage (stage 11; [21]).

2.4 Indirect immunofluorescence

The embryos were fixed and treated as previously described (Hatte *et al.*, 2014). Briefly, embryos were fixed with 2% trichloroacetic acid in 1× F1 buffer. After embryos were devitellinated, cells were permeabilised in PBS+1% Triton X-100 for 20 min at room temperature, incubated in PBS+0.1% Triton X-100 (PBST 0.1%) for 10 min and then blocked for 1 h in 2% BSA in PBST 0.1% (BSA-PBST). Embryos were incubated overnight in BSA-PBST at 14°C with a primary antibody.

The primary antibodies used in this study are directed against C-cadherin (DHSB, 6B6, 1:200), α-catenin (ThermoFisher Scientific, PA1-25081, 1:100), β-catenin (Santa-Cruz, SC-7199,1:100), F-actin (AC-40, Sigma, 1:200), phospho S20 myosin regulatory light chain (MRLC, pS19 in *Xenopus laevis*, abcam, ab2480, 1:100), MKLP1 (Santa Cruz, SC-867, 1:100), Ect2 (Millipore 1:100), *Xenopus laevis* anillin and myosin heavy chain A (MHCA) (a kind gift from Aaron Straight, [4], 1:100), *Xenopus laevis* Rock II (a kind gift from Johné Liu, [19] 1:100), ZO-1 (Zymed, 33-9100, 1:200), occludin (a kind gift from Sandra Citi [22], 1:100), GFP (Roche, clone 7.1 and 13.1, 11914460001, 1:100) and mcherry (abcam, ab167453, 1:200).

After washing with PBST 0.1%, embryos were incubated with Alexa Fluor-488 or-555 anti-mouse, anti-rabbit or anti-sheep (ThermoFisher Scientific) and TO-PRO-3 to stain DNA (Invitrogen, 0.5 µg/ml) in BSA-PBST for 1 h at room temperature. After 3 washes of 5 min in 0.1% PBST, embryos were mounted in Vectashield (Vector).

For F-actin staining, embryos were fixed in 3.7% formaldehyde in F1 buffer for 2 hours at room temperature, permeabilised and blocked as previously described. After blocking, embryos were incubated with AlexaFluor 555-conjugated Phalloidin (Life Technologies, 1 U/ml) and TO-PRO3 for 2 h, washed and mounted in Vectashield.

2.5 Lambda phosphatase treatment of embryos

Embryos fixed in TCA, as previously described, were incubated in the appropriate buffer with or without 25 units of lambda phosphatase (New England Biolabs) at 30°C for 30 min. Embryos were then extensively washed with PBS, permeabilized and proceed for indirect immunofluorescence with the anti-phospho S20 myosin regulatory light chain as the primary antibody.

2.6 Confocal microscopy on living and fixed embryos

For immunofluorescence, a Leica SP5 confocal microscope with an oil immersion objective 40x / 1.25-0.75 HC PL APO (WD 0.1 mm) was used. Imaging of live embryos was performed with a Leica SP8 confocal microscope with a 63x / 1.4 HC PL APO oil objective, using a resonant scanner. This scanner allows extremely fast acquisitions (scanning frequency of 8000 Hz), essential for analyzing the recruitment of proteins into the contractile ring.

2.7 Quantification of immunolabelling at adherens and tight junctions

To test if contractile ring activation could be polarized along the apical-basal cell axis, the fluorescence intensities of Rock II and pS19MRLC detected by immunolabelling in fixed embryos were quantified. Because Rock II localises at the apical junctional complex and is distributed along the lateral membrane several µm below (Fig. 1B), quantification of fluorescence intensity was standardized by measuring 10 µm below the apical cell-cell junctions. At this distance, the fluorescence intensity was minimal. In contrast, pS19MRLC fluorescence is more restricted to apical cell-cell contacts compared to Rock II (Fig. 1B), therefore quantification was standardized by measuring 5 µm below apical junctions. For both Rock II and pS19MRLC,

fluorescence intensities were also measured at non-furrowing faces, orthogonal to the division site (hereafter referred as cell poles). To quantify fluorescence intensity for Rock II and pS19MRLC, the mean pixel intensity was measured in a region of interest (ROI) at the cell-cell contacts. This ROI was placed at the division site for cells already engaged in cytokinesis or perpendicularly and equally distant from mitotic chromosomes. The mean fluorescence pixel intensity in proximity to the presumptive division site was measured in a ROI with identical size to the ROI used for quantification at the division site and was subtracted from the pixel intensity at the division site.

2.9 Quantification of the duration of ring contraction and contractile ring formation

The duration of the ring contraction was calculated by subtracting the time when the contractile ring begins to contract at the basal side to the time when it is fully ingressed and concentrates at the apical pole of the cell. For the duration of the contractile ring formation, the time when the protein of interest begins to accumulate at the presumptive division site was subtracted from the time when the contractile ring begins to constrict at the basal side.

2.10 Image processing and quantification

Images were processed using ImageJ software (Rasband, W.S., http://rsb.info.nih.gov/ij) and figures were prepared using ImageJ and Photoshop. Graphing was performed using Microsoft Excel. Kymographs of lateral cell-cell contacts were mounted manually.

2.11 Statistical analysis

No statistical method was used to predetermine the sample size. The experiments were not randomized and investigators were not blinded to allocation during experiments and outcome assessment. Experiments were repeated at least two times. Sample sizes are indicated for each experiment in figure legends. A two-tailed unpaired Student t-test was applied to determine statistical significance. Statistical analysis was performed using Microsoft Excel software except for Rock II and

Journal Pre-proof

pS19MRLC fluorescence pixel intensities at the division sites and poles for which a Mann Whitney test was done using Prism software.

3. Results

3.1 The proteins involved in cytokinesis localize at the apical junctional complex in the Xenopus laevis embryo

First and foremost, we studied the formation of the actomyosin contractile ring by examining the localization of several proteins involved in cytokinesis in the epithelium of *Xenopus laevis* embryo. In non-dividing cells, filamentous actin (F-actin) and myosin heavy chain A (MHCA) localize at apical cell-cell contacts where they form a contractile belt at the apical cell periphery (Fig. 1A). On orthogonal projections, proteins appear as dots extended by faint signals which intensity decreases along the lateral cell-cell contacts (Fig. 1A, arrowheads on orthogonal views). The F-actin signal decreases along the lateral cell cortex whereas β-catenin was localized all around the basolateral cell contacts (Fig. 1B; [23]) indicating that the decrease of F-actin signal is specific. MHCA was also detected in the cytoplasm and at the medial cortex. Anillin, a scaffolding protein which interacts with F-actin and myosin, also localise at the apical cell-cell contacts and into nuclei (Fig. 1A), as described previously [3]. As previously shown in cultured cells [24], the two regulators of cytokinesis, MKLP1, a constituent of the centralspindlin complex and Ect2, an activator of Rho GTPase, localize at apical cell-cell contacts (Fig. S1A and S1C). We also examined the localisation of the protein kinase Rock II which activates myosin by phosphorylating the serine 20 residue (serine 19 in *Xenopus laevis*) of the myosin regulatory light chain (MRLC) leading to the contraction of the actomyosin contractile ring during cytokinesis [25]. The activated MRLC was detected with an antibody recognizing the MRLC serine 19 phosphorylation (pS19MRLC). Both proteins, Rock II and activated myosin, co-localize with C-cadherin at the adherens junctions, although pS19MRLC was more restricted towards apical side unlike Rock II (Fig. 1C).

Our results show that all the key proteins involved in cytokinesis that we examined localize to the apical cell-cell contacts in the *Xenopus* embryo epithelium.

3.2 Accumulation of contractile ring components begins at apical cell-cell contacts and expands basally along the lateral membrane

To study the formation dynamics of the actomyosin contractile ring in epithelial cells, we expressed four distinct fluorescent proteins in embryos. We expressed the two proteins involved in cytokinesis, Rock II K/R, a catalytically inactive form of Rock II and anillin tagged with GFP (respectively GFP-Rock II K/R and 3xGFP-anillin) and used two fluorescent probes: the SF9-GFP intrabody, which detects the endogenous myosin heavy chain A (MHCA) [26], and GFP-Lifeact which detects F-actin [27]. As described above for endogenous proteins, all the four proteins localized at the apical cell-cell junctions (Fig. 2 A-D and Fig. S2A). Expression of these fluorescent proteins has no significant impact on the duration of ring contraction compared with cells expressing GFP fused with a glycosylphosphatidylinositol (GPI)-anchor (GFP-GPI) used to visualize cells plasma membrane (Fig. S2B, mean duration of ring contraction 5 min 50 s). During cytokinesis, the four proteins that we tested localize at the contractile ring (Fig. 2A-D, white arrowheads on front views, see Fig. S2C for an example of full cytokinesis and asymmetric constriction of the contractile ring in a cell expressing 3xGFP-anillin). Interestingly, very shortly before plasma membrane ingression starts at the basal side, the fluorescence intensity of the four proteins increases at the apical cell-cell contacts at the presumptive plasma membrane ingression site (Fig. 2 A-D, dashed circles on front views, orthogonal views). The extent to which fluorescence intensities increased depended on the fluorescent protein, with 3xGFP-anillin increasing more than the 3 others (Fig. 2 A-D, histograms). Subsequently, fluorescence spreads and fluorescence intensity increases with time along the baso-lateral membrane (Fig. 2 A-D, kymographs and histograms). The time elapsed between the beginning of accumulation of the four proteins at the apical cell-cell contacts and the beginning of plasma membrane ingression at the basal side ranges from 12 s. to 55 s. (Fig 2E, mean time: 30 seconds). Such a dynamic localization does not occur for GFP-GPI nor for the tight junction protein ZO-1, which follows the plasma membrane shape modifications without additional accumulation compared to non-dividing cells (Fig. S3A and S3B).

Journal Pre-proof

In epithelial cells of the *Xenopus* embryos, the mitotic spindle position along the apicobasal axis is stereotypically biased toward the apical surface (Fig. S4 and [23]). Because in late anaphase, the mitotic spindle signals to the cell cortex the position of the contractile ring, the asymmetrically positioned mitotic spindle could be involved in the apical-to-basal accumulation of contractile ring proteins. Interestingly, the two cytokinesis regulators, MKLP1 and Ect2, localized at apical and lateral cell-cell contacts in anaphase cells (Fig. S1B and S1D, respectively). This result suggests that the asymmetrically positioned mitotic spindle could drive the apical recruitment of the contractile ring proteins.

In summary, the four proteins involved in cytokinesis, which we examined, start to accumulate at the presumptive division site asymmetrically from the apical cell-cell contacts and expand along the lateral cell plasma membrane towards the basal side.

3.3 Activation of the actomyosin contractile ring is polarized

The finding that contractile ring components accumulate asymmetrically led to the question of whether activation of the actomyosin contractile ring could be polarized along the apical-basal cell axis. Since RhoA is a master regulator of actomyosin ring activation, we thought to use the GFP-rGBD probe [28] to follow active RhoA in living embryos. Fluorescence of the GFP-rGBD probe was detected at cell-cell contacts in non-dividing cells and at the contractile ring in cells advanced in cytokinesis (Fig. S5A). However, the fluorescence in the cytoplasm was also high (cells expressing high and low levels of GFP-rGBD are shown in Fig. S5A) which turned out to be incompatible with the high temporal resolution needed to image GFP-rGBD at the presumptive division site. This issue made the GFP-rGBD probe unusable for our study on the early steps of cytokinesis. To overcome this challenge, we investigated the localization of the myosin II regulatory light chain phosphorylated on serine 19 (pS19MRLC) in fixed embryos. S19 phosphorylation, which is catalysed by Rock II, induces myosin activation and subsequently actomyosin constriction. To validate the approach based on fixed material, we first studied Rock II localization, as we have previously shown the polarized accumulation of GFP-Rock II KR at the presumptive division site. Immunofluorescence signal of Rock II was indistinguishable between cells in metaphase and at the very beginning of anaphase, when chromosomes start

splitting (these cells will be referred as early anaphase, Fig. 3A). However, in cells more advanced in anaphase, Rock II signal was detected deeper along the lateral plasma membrane. Hereafter, these cells advanced in anaphase, showing Rock II accumulation but without any sign of plasma membrane ingression will be referred as early cytokinesis (Fig. 3A, compare orthogonal views at the division site of early anaphase with early cytokinesis). In cells more advanced in cytokinesis, the ingressed plasma membrane was generally fully labelled by the anti-Rock II antibody (Fig. 3A). However, for some unknown reason, we also frequently observed incomplete labelling at the base of the contractile ring. A similar observation of incomplete ring labelling was previously reported in living tissues of *Drosophila* [29]. Rock II fluorescence intensity was quantified at the presumptive division site in early anaphase and early cytokinesis cells. For comparison, in the same cells, we also quantified Rock II signal at the cell poles (non-furrowing faces orthogonal to the division site). The quantitative analysis shows a significant statistical difference between Rock II intensity at the presumptive division site compared to cell poles (Fig. 3B). Moreover, at the presumptive division site, Rock II signal intensity increases with the length of plasma membrane labelled for Rock II (Fig. 3C). Although Rock II signal intensity also increases at the cell poles, this increase was less marked compared to the presumptive division site (Fig. 3C, equation of linear regressions are given for poles and division site). The correlation between Rock II accumulation and the length of the plasma membrane labelled for Rock II suggests that the Rock II signal expands along the baso-lateral membrane. This result is in agreement with the previously shown polarized accumulation of the GFP-Rock II K/R probe in living embryos. Therefore, we used indirect immunofluorescence with fixed embryos to study myosin activation.

Fixed embryos were labelled with an anti-pS19 MRLC antibody, the specificity of which was previously validated (Fig. S5B). As previously observed for Rock II, pS19MRLC signal was indistinguishable between cells in metaphase and early anaphase (Fig. 3D). As previously quantified for Rock II, fluorescence intensities were also quantified at the division site and at the cell poles. Quantifications show a significant statistical difference between pS19MRLC fluorescence intensity at the presumptive division site compared to cell poles (Fig. 3E). Moreover, pS19MRLC signal intensity increases with the length of the plasma membrane labelled for

pS19MRLC at the presumptive cell division site whereas it remained almost unchanged at the cell poles (Fig. 3F). These results are consistent with the phosphorylation of the myosin regulatory light chain being polarized, starting at the apical cell-cell junctions and spreading along the lateral membrane towards the basal side.

Altogether, our results show that accumulation of proteins constituting the actomyosin contractile ring, and activation of the ring start at the apical cell-cell contacts and expands along the lateral membrane. Since furrowing progresses in the basal to apical orientation, the reverse polarity of the contractile ring formation was unexpected.

3.4 The adherens junctions are involved in the polarized formation of the contractile ring

Our results show that cytokinetic proteins co-localise with adherens junctions and the assembly and activation of the cytokinetic contractile ring begins at the apical cell-cell contacts. Due to the close link previously shown between cytokinesis and the adherens junctions [12,13,28,29, 35], we examined if adherens junctions could be involved in the asymmetric formation of the contractile ring.

To interfere with the adherens junctions, we followed two distinct approaches. In the first approach, we used a deletion mutant corresponding to the cytosolic domain of C-cadherin (Ctail) [16]. C-cadherin (also termed EP-cadherin) is the main adherens junctions molecule of the *Xenopus* gastrula [31,32]. Because the extra-cellular and the trans-membrane domains are missing in the Ctail, it is unable to integrate the plasma membrane and bridge with C-cadherin of neighbouring cells. However, the cytosolic domain of E-cadherin is responsible for indirect binding with the F-actin *via* interaction with α and β catenins. It has been shown that the ubiquitous expression in the *Xenopus* embryos of high levels of Ctail provokes cell dissociation [16]. This loss of cell-cell contacts indicated a decrease in cell adhesion suggesting that the Ctail could act as a dominant-negative mutant by titrating catenins. Because the mode of action of Ctail was not described in details, we further characterized this mutant. The Ctail mutant was co-expressed together with GFP or RFP -GPI used as tracers, and we examined the expression of diverse proteins localized at the adherens junctions.

Unlike control cells, the apical membrane of cells expressing Ctail was frequently round (Fig. 4A, compare orthogonal views of control and Ctail), suggesting a decrease in cell-cell adhesion as previously reported by Lee and Gumbiner [16]. The amounts of endogenous C-cadherin, α and β-catenins, F-actin and Rock II, localized at the adherens junctions, were significantly decreased in cells expressing Ctail (Fig. 4A, histograms). In contrast, localization of two constituents of the tight junctions, ZO-1 and occludin, was not affected (Fig. S6). Our results show that expression of Ctail disrupts the adherens junctions, which could explain epithelial structural defects observed in our and previous studies [16].

We then tested if the expression of the Ctail mutant could affect the formation and contraction of the actomyosin ring. In both control and Ctail expressing cells, Lifeact-GFP and 3xGFP-anillin fluorescence appears apically and expands along the lateral membrane (Fig. 4B and 4D, upper rows). The asymmetric contraction of the actomyosin ring from the basal side towards the apical side was also unaffected by Ctail expression (Fig. 4B and 4D, lower rows).

Interestingly, the time elapsed between the beginning of the accumulation of Lifeact-GFP and 3xGFP-Anillin at the apical cell-cell contacts and the beginning of plasma membrane ingression at the basal side significantly increased in Ctail expressing cells compared to controls (58.9+/-7.2 s vs 30.7+/-10.4 s for Lifeact-GFP and 54.2+/-13.1 s vs 21.4+/-5.9 s for 3xGFP-Anillin, respectively Fig. 4C and 4E). This result suggested that the adherens junctions could be involved in the polarized recruitment of the contractile ring components. To test this hypothesis, we followed a second approach to interfere with the adherens junctions.

In the second approach, we used an antisense morpholino oligonucleotide to deplete α-catenin, which indirectly links C-cadherin to the actomyosin cytoskeleton (Mo α-cat, Fig. 5A). As previously shown [20,33], depletion of α-catenin also led to a significant decrease of C-cadherin (Fig. 5A) and perijunctional actin filaments (not shown, [17]). This result shows that Mo α-cat, by depleting α-cat, destabilizes the adherens junctions. Measurement of the time lasting from the beginning of fluorescence increase and the start of ring constriction shows that the recruitment durations of Lifeact-GFP and 3xGFP-anillin at the apical cell-cell contacts significantly increases in Mo α-cat treated cells compared with control morpholino (MoCo) cells (57.3+/-13.0 s vs 33.1+/-11.0 s for Lifeact-GFP and 41.5+/-8.0 s vs 27.6+/-4.0 s, respectively Fig.

5B and 5C, histograms). As with the Ctail mutant, the polarized recruitment of Lifeact-GFP and 3xGFP-anillin occurred in cells treated with MoCo as well as cells treated with Mo α-cat (Fig. 5B and 5C). The subsequent asymmetric ring constriction also normally occurred (not shown and [17] for Lifeact-GFP). To test if tight junctions may contribute in maintaining the asymmetric ring constriction in α-cat depleted cells, embryos were microinjected with Mo α-cat, Mo ZO-1 and 3xGFP-anillin mRNA. ZO-1 is a tight junction-associated protein. As previously shown with ZO-1 disruption alone [17], disruption of tight and adherens junctions led to prolonged cytokinesis and flattened contractile ring with normal asymmetry (Fig. S7).

Altogether, these results indicate that the adherens junctions are involved in the polarized accumulation of the contractile ring components at the presumptive division site.

4. Discussion

In the present study, we have shown that at cytokinesis onset the levels of proteins forming and activating the contractile actomyosin ring increase at the apical cell-cell contacts. The initiation of ring formation at the apical contacts could appear in contradiction with the asymmetric furrowing which progresses from the basal side towards the apical side. However, our results show that the ring formation is extremely rapid, occurring in approximatively 30 seconds before the first sign of ring constriction. Moreover, we have shown that ring formation spread laterally from apical contacts towards the basal side of cells.

Cytokinesis by asymmetric furrow ingression is closely linked to the presence of an apical junctional complex in epithelial cells. Indeed, the actomyosin contractile ring remains associated with apically localized adherens junctions in *Drosophila* [12,13]. In vertebrates, the apical junctional complex continuously contacts the contractile ring [34–36]. Moreover, in *Drosophila*, it has been shown that interfering with the adherens junctions causes the furrow to become symmetric [12,13]. Although these observations showed that the contractile ring is associated with the adherens junctions, they did not elucidate when the two structures become associated. In the

present study, we show that the adherens junctions are involved in the polarized contractile ring formation.

Although interfering with adherens junctions increased the duration of accumulation of proteins forming the contractile ring, it did not abolish the asymmetric contraction of the ring. These results are in contrast with previous studies in *Drosophila* in which it was shown that knockdown by RNAi of E-cadherin and α-catenin or in armadillo (the *Drosophila* orthologue of β-catenin) mutant, constriction of the actomyosin ring becomes symmetric [12,13]. The remaining amounts of junctional proteins at the adherens junctions observed in Ctail expressing cells and α-catenin knocked down cells could be sufficient to maintain asymmetric constriction of the contractile ring as noticed in our study. However, in Ctail cells, we frequently observed a rounding of cell indicative of a decrease in cell adhesion, which should have affected the asymmetric furrowing. The discrepancy between our results and results obtained in *Drosophila* regarding the asymmetric ring constriction may originate from the distinct models used. The organization of adherens and tight (septate in *Drosophila*) junctions differ in vertebrates and insects. Moreover, cytokinesis also exhibit marked difference in the two models including the maintenance of contacts of apical junctions with the contractile ring [35]. It is possible that the tight junctions, by maintaining mechanical strain on the cell plasma membrane, could be involved in the maintenance of asymmetric constriction of the contractile ring. In this respect, we observed that tight junctions were unaffected by expression of the Ctail mutant. The double disruption of tight and adherens junctions led to flattened contractile ring and altered cytokinesis duration (Fig. S7), as previously shown for tight junction disruption alone which increases mechanical tension applied on adherens junctions [17]. In the double knockdown, it is possible that ZO-1 depletion could lead, *via* remaining adherens junction proteins, to an increase of mechanical tension applied on adherens junctions and normal ring contraction asymmetry. As the mechanism leading to the increase of mechanical tension applied to adherens junctions upon ZO-1 depletion is unknown, the hypothesis of tight junctions involvement in asymmetric contraction of the contractile ring will require further investigations.

In epithelial cells of *Xenopus* embryos, the mitotic spindle position is stereotypically biased toward the apical cell side [23] and (Fig. S4). This result suggests that the asymmetric apicobasal position of the mitotic spindle could be involved in

accumulation of contractile ring proteins starting at apical cell-cell contacts of the presumptive division site. Our results suggest that in dividing epithelial cells, the signalling pathway leading to the contractile ring activation could be focused on adherens junctions (Fig. 5D). As microtubules are known to be involved in the signalling which induces cytokinesis [1], it will be of interest to explore their putative implication in the polarized accumulation of contractile ring proteins.

Interestingly, all proteins involved in cytokinesis analysed in the present study localize at the apical cell-cell contacts before cytokinesis onset. The previous studies showing that the centralspindlin complex, Ect2 and anillin regulate the Rho GTPase cycle at the adherens junctions indicated that they could participate in apical junctions' homeostasis [3,24,37]. Conversely, it has been shown that depletion of α-catenin in MCF-7 epithelial cells reduces Ect2 levels at the adherens junctions [24], indicating that the adherens junctions are involved in recruiting components involved in the actomyosin contractility of the perijunctional belt in non-dividing cells. Consequently, our results showing that adherens junctions are involved in the ring formation extend their implication to the contractile ring components during cytokinesis. Additional studies will be required to understand in details the highly dynamic mechanisms supporting the recruitment of cytokinetic proteins at the onset of epithelial cell cytokinesis.

Studies of cytokinesis in epithelial tissues have revealed the basal to the apical asymmetry of the contractile ring contraction. However, before contraction, the cell plasma membrane and the underneath contractile ring need to be freed from extracellular contacts at their basal side [38–40]. Our study raises the question of how epithelial cells precisely orchestrate polarized contractile ring formation and activation with basal membrane disengagement.

5. Conclusions

Our study highlight the involvement of adherens junctions in the polarized formation and activation of the actomyosin contractile ring at the onset of cytokinesis. Our results give a simple explanation to the previously reported association of the actomyosin contractile ring with apical junctional complex during cytokinesis.

Acknowledgements

We are grateful to Michael Danilchik, Arun Prasath Damodaran (C. Prigent's team) and Roland Le Borgne for critical reading on the manuscript. We thank the Microscopy Rennes Imaging Center (MRic, BIOSIT, IBiSA). This work was supported by the Centre National de la Recherche Scientifique (CNRS) and the Ligue Contre le Cancer (comités 29 et 35). G.H. was supported by the Ministère de l'Enseignement Supérieur, de la Recherche et de l'Innovation and partly by a grant from the Ligue Nationale Contre le Cancer.

Author contributions

G.H. carried out the experiments, generated and interpreted the data. J-P.T. designed research and supervised the project. G.H. C.P. and J-P. T. wrote the manuscript.

Conflict of interest

The authors declare no conflict of interest.

References

[1] P.P. D'Avino, M.G. Giansanti, M. Petronczki, Cytokinesis in animal cells, Cold Spring Harb. Perspect. Biol. 7 (2015). https://doi.org/10.1101/cshperspect.a015834.

[2] A.J. Piekny, M. Glotzer, Anillin Is a Scaffold Protein That Links RhoA, Actin, and Myosin during Cytokinesis, Curr. Biol. (2008). https://doi.org/10.1016/j.cub.2007.11.068.

Journal Pre-proof

[3] C.C. Reyes, M. Jin, E.B. Breznau, R. Espino, R. Delgado-Gonzalo, A.B. Goryachev, A.L. Miller, Anillin regulates cell-cell junction integrity by organizing junctional accumulation of Rho-GTP and actomyosin, Curr. Biol. (2014). https://doi.org/10.1016/j.cub.2014.04.021.

[4] A.F. Straight, C.M. Field, T.J. Mitchison, Anillin binds nonmuscle myosin II and regulates the contractile ring, Mol. Biol. Cell. 16 (2005). https://doi.org/10.1091/mbc.E04-08-0758.

[5] J. Liu, G.D. Fairn, D.F. Ceccarelli, F. Sicheri, A. Wilde, Cleavage furrow organization requires PIP 2-mediated recruitment of anillin, Curr. Biol. (2012). https://doi.org/10.1016/j.cub.2011.11.040.

[6] S. Le Bras, R. Le Borgne, Epithelial cell division - Multiplying without losing touch, J. Cell Sci. (2014). https://doi.org/10.1242/jcs.151472.

[7] J.P. Tassan, M. Wühr, G. Hatte, J. Kubiak, Asymmetries in cell division, cell size, and furrowing in the xenopus laevis embryo, in: Results Probl. Cell Differ., 2017. https://doi.org/10.1007/978-3-319-53150-2_11.

[8] M.C. Gibson, N. Perrimon, Apicobasal polarization: Epithelial form and function, Curr. Opin. Cell Biol. (2003). https://doi.org/10.1016/j.ceb.2003.10.008.

[9] E. Rodriguez-Boulan, I.G. Macara, Organization and execution of the epithelial polarity programme, Nat. Rev. Mol. Cell Biol. (2014). https://doi.org/10.1038/nrm3775.

[10] U. Tepass, The apical polarity protein network in drosophila epithelial cells: Regulation of polarity, junctions, morphogenesis, cell growth, and survival, Annu. Rev. Cell Dev. Biol. (2012). https://doi.org/10.1146/annurev-cellbio-092910-154033.

[11] B.J. Thompson, Cell polarity: Models and mechanisms from yeast, worms and flies, Dev. (2013). https://doi.org/10.1242/dev.083634.

[12] E. Morais-De-Sá, C. Sunkel, Adherens junctions determine the apical position of the midbody during follicular epithelial cell division, EMBO Rep. (2013). https://doi.org/10.1038/embor.2013.85.

[13] C. Guillot, T. Lecuit, Adhesion Disengagement Uncouples Intrinsic and Extrinsic Forces to Drive Cytokinesis in Epithelial Tissues, Dev. Cell. (2013). https://doi.org/10.1016/j.devcel.2013.01.010.

[14] A.D. Chalmers, B. Strauss, N. Papalopulu, Oriented cell divisions asymmetrically segregate aPKC and generate cell fate diversity in the early Xenopus embryo, Development. (2003). https://doi.org/10.1242/dev.00490.

[15] Y. Le Page, I. Chartrain, C. Badouel, J.-P. Tassan, A functional analysis of MELK in cell division reveals a transition in the mode of cytokinesis during Xenopus development, J. Cell Sci. 124 (2011). https://doi.org/10.1242/jcs.069567.

[16] C.H. Lee, B.M. Gumbiner, Disruption of gastrulation movements in Xenopus by a dominant-negative mutant for C-cadherin, Dev. Biol. (1995). https://doi.org/10.1006/dbio.1995.1288.

[17] G. Hatte, C. Prigent, J.-P. Tassan, Tight junctions negatively regulate mechanical forces applied to adherens junctions in vertebrate epithelial tissue, J. Cell Sci. 131 (2018). https://doi.org/10.1242/jcs.208736.

[18] G. Hatte, M. Tramier, C. Prigent, J.P. Tassan, Epithelial cell division in the Xenopus laevis embryo during gastrulation, Int. J. Dev. Biol. (2014). https://doi.org/10.1387/ijdb.140277jt.

[19] S. Farah, Y. Agazie, N. Ohan, J.K. Ngsee, X.J. Liu, A Rho-associated protein kinase, ROKα, binds insulin receptor substrate-1 and modulates insulin signaling, J. Biol. Chem. (1998). https://doi.org/10.1074/jbc.273.8.4740.

[20] S. Nandadasa, Q. Tao, A. Shoemaker, S. wook Cha, C. Wylie, Regulation of classical cadherin membrane expression and F-actin assembly by alpha-catenins, during Xenopus embryogenesis, PLoS One. (2012). https://doi.org/10.1371/journal.pone.0038756.

[21] P.D. Nieuwkoop, J. Faber, Normal Table of Xenopus laevis (Daudin)., North-Holl, Amsterdam, 1967.

[22] M. Corderionsi, E. Mazzon, L. De Rigo, S. Baraldo, F. Meggio, S. Citi, Occludin dephosphorylation in early development of Xenopus laevis, J. Cell Sci. (1997).

[23] S. Woolner, N. Papalopulu, Spindle Position in Symmetric Cell Divisions during Epiboly Is Controlled by Opposing and Dynamic Apicobasal Forces, Dev. Cell. (2012). https://doi.org/10.1016/j.devcel.2012.01.002.

[24] A. Ratheesh, G.A. Gomez, R. Priya, S. Verma, E.M. Kovacs, K. Jiang, N.H. Brown, A. Akhmanova, S.J. Stehbens, A.S. Yap, Centralspindlin and α-catenin regulate Rho signalling at the epithelial zonula adherens, Nat. Cell Biol. (2012). https://doi.org/10.1038/ncb2532.

[25] M. Amano, M. Ito, K. Kimura, Y. Fukata, K. Chihara, T. Nakano, Y. Matsuura, K. Kaibuchi, Phosphorylation and activation of myosin by Rho-associated kinase (Rho- kinase), J. Biol. Chem. (1996). https://doi.org/10.1074/jbc.271.34.20246.

[26] C. Nizak, S. Martin-Lluesma, S. Moutel, A. Roux, T.E. Kreis, B. Goud, F. Perez, Recombinant antibodies against subcellular fractions used to track endogenous Golgi protein dynamics in vivo, Traffic. (2003). https://doi.org/10.1034/j.1600-0854.2003.00132.x.

[27] J. Riedl, A.H. Crevenna, K. Kessenbrock, J.H. Yu, D. Neukirchen, M. Bista, F. Bradke, D. Jenne, T.A. Holak, Z. Werb, M. Sixt, R. Wedlich-Soldner, Lifeact: A versatile marker to visualize F-actin, Nat. Methods. (2008). https://doi.org/10.1038/nmeth.1220.

[28] H.A. Benink, W.M. Bement, Concentric zones of active RhoA and Cdc42 around single cell wounds, J. Cell Biol. (2005). https://doi.org/10.1083/jcb.200411109.

[29] N. Founounou, N. Loyer, R. Le Borgne, Septins Regulate the Contractility of the Actomyosin Ring to Enable Adherens Junction Remodeling during Cytokinesis of Epithelial Cells, Dev. Cell. 24 (2013) 242–255. https://doi.org/10.1016/j.devcel.2013.01.008.

[30] S. Herszterg, A. Leibfried, F. Bosveld, C. Martin, Y. Bellaiche, Interplay between the Dividing Cell and Its Neighbors Regulates Adherens Junction Formation during Cytokinesis in Epithelial Tissue, Dev. Cell. 24 (2013) 256–270. https://doi.org/10.1016/j.devcel.2012.11.019.

[31] Y.S. Choi, R. Sehgal, P. McCrea, B. Gumbiner, A cadherin-like protein in eggs

Journal Pre-proof

and cleaving embryos of Xenopus laevis is expressed in oocytes in response to progesterone, J. Cell Biol. (1990). https://doi.org/10.1083/jcb.110.5.1575.

[32] D. Ginsberg, D. DeSimone, B. Geiger, Expression of a novel cadherin (EP-cadherin) in unfertilized eggs and early Xenopus embryos, Development. (1991).

[33] G. Hatte, C. Prigent, J.P. Tassan, Tight junctions negatively regulate mechanical forces applied to adherens junctions in vertebrate epithelial tissue, J. Cell Sci. (2018). https://doi.org/10.1242/jcs.208736.

[34] J. Baker, D. Garrod, Epithelial cells retain junctions during mitosis., J. Cell Sci. 104 (Pt 2 (1993) 415–425.

[35] T. Higashi, T.R. Arnold, R.E. Stephenson, K.M. Dinshaw, A.L. Miller, Maintenance of the Epithelial Barrier and Remodeling of Cell-Cell Junctions during Cytokinesis, Curr. Biol. 26 (2016) 1829–1842. https://doi.org/10.1016/j.cub.2016.05.036.

[36] Y. Jinguji, H. Ishikawa, Electron microscopic observations on the maintenance of the tight junction during cell division in the epithelium of the mouse small intestine., Cell Struct. Funct. 17 (1992) 27–37. http://www.ncbi.nlm.nih.gov/pubmed/1586965.

[37] A. Rosa, E. Vlassaks, F. Pichaud, B. Baum, Ect2/Pbl Acts via Rho and Polarity Proteins to Direct the Assembly of an Isotropic Actomyosin Cortex upon Mitotic Entry, Dev. Cell. (2015). https://doi.org/10.1016/j.devcel.2015.01.012.

[38] K.G. Bourdages, B. Lacroix, J.F. Dorn, C.P. Descovich, A.S. Maddox, Quantitative analysis of cytokinesis In Situduring C. Elegans postembryonic development, PLoS One. (2014). https://doi.org/10.1371/journal.pone.0110689.

[39] D.J. Fishkind, Y.L. Wang, Orientation and three-dimensional organization of actin filaments in dividing cultured cells, J. Cell Biol. (1993). https://doi.org/10.1083/jcb.123.4.837.

[40] N. Taneja, A.M. Fenix, L. Rathbun, B.A. Millis, M.J. Tyska, H. Hehnly, D.T. Burnette, Focal adhesions control cleavage furrow shape and spindle tilt during mitosis, Sci. Rep. (2016). https://doi.org/10.1038/srep29846.

1

2

Journal Pre-proof

Journal Pre-proof

Figure Legends

Fig. 1. Proteins involved in cytokinesis localize at the apical junctional complex. (A) F-actin was detected with fluorescent phalloidin and myosin heavy chain A (MHCA) and anillin by indirect immunofluorescence with specific antibodies. DNA stained with TO-PRO-3 is shown in inset. Orthogonal projections along the dashed lines are shown below apical views. Arrowheads point to the concentration of the labelling at the apical and lateral junctions. (B) Orthogonal projections of cells labelled by indirect immunofluorescence of F-actin and β-catenin. DNA stained with TO-PRO-3 (grey) was merged with F-actin and β-catenin. Arrowheads point to the concentration of the labelling at the apical and lateral junctions. (C) Co-labelling by indirect immunofluorescence of Rock II and phosphorylated S19MRLC (pS19MRLC, activated myosin) with the adherens junctional protein C-cadherin. The confocal planes passing through the apical junctions and overlays are shown. Orthogonal projections along the dashed lines are shown. Arrowheads point to the concentration of the labelling at the apical junctions. Scale bars: 10 µm.

Fig. 2. Accumulation of cytokinetic proteins begins at the apical junctions and further spreads basally along the lateral plasma membrane.
Lifeact-GFP (A), SF9-GFP (B), 3xGFP-anillin (C) and GFP-Rock II KR (D) were expressed in living embryos and imaged. For each fluorescent protein, the representative still images of a dividing cell are shown. Time 0 corresponds to the start of fluorescent protein accumulation at the apical cell-cell contacts (time is indicated in seconds). Black arrowheads indicate ring contraction onset at the basal side. White arrowheads points on the accumulation of fluorescent proteins at the contractile ring. Below: orthogonal projections of a single lateral cell-cell contact (indicated by a dotted circle in front views) from the onset of fluorescent protein accumulation to the onset of ring contraction. Histograms show relative fluorescence intensity vs cell-cell contacts length at the onset of fluorescent protein accumulation (blue) and at the onset of ring contraction (red). a. : apical, b. : basal. ***: p-values < 0.001. Scale bars: 10 µm. (E) Duration of cytokinetic proteins accumulation at the division site. The time between the onset of proteins accumulation and actomyosin

ring constriction was measured for the four fluorescent proteins. The number of cells analysed for Lifeact-GFP, SF9-GFP, 3xGFP-anillin and GFP-Rock II KR are respectively 11, 9, 17 and 11. Standard deviations are indicated.

Fig. 3. Activation of the actomyosin contractile ring is polarized.
Indirect immunofluorescence for Rock II (A) and pS19MRLC (D). Surface views (Z0) and confocal planes 10 and 5 µm below are shown for respectively Rock II and pS19MRLC. Inset shows DNA detected with TO-PRO-3. Cells in metaphase, early anaphase, cytokinesis onset and advanced cytokinesis are presented for each antibody used. Orthogonal projection along the dashed lines are shown below. The horizontal and vertical dashed lines (shown only for metaphase cells) indicate the plane used to obtain orthogonal projection, respectively at the division sites and at the poles. Histograms B and E show pixel intensity of respectively Rock II and pS19MRLC fluorescence at the division site (blue circles) and poles (orange circles). The positions where the fluorescence intensity was measured are marked by blue (division site) and orange (poles) arrowheads on orthogonal projections. n= 50 for Rock II and 45 for pS19MRLC. Histograms C and F show pixel intensity of respectively Rock II and pS19MRLC fluorescence at the division site (blue circles) and poles (orange circles) as a function of the length of the lateral cell-cell contact labelled for respectively Rock II and pS19MRLC. Equations of the linear regressions are specified in the top right corner. Scale bars:10 µm.

Fig. 4. Destabilization of the adherens junctions increases the duration of cytokinetic proteins accumulation but does not impact the polarity of cytokinetic proteins recruitment and asymmetric ring constriction.
(A) Expression of the C-cadherin deletion mutant, Ctail, destabilizes adherens junctions. Embryos expressing GFP-gpi or RFP-gpi alone (control) and co-expressing Ctail with GFP-gpi or RFP-gpi used as tracers were fixed and processed for indirect immunofluorescence with antibodies against C-cadherin, α and β-catenins and Rock II or with fluorescent phalloidin (to detect F-actin). GFP-gpi and RFP-gpi tracers were detected by immunofluorescence with antibodies against GFP and RFP, respectively. Apical confocal planes and orthogonal projections are shown. DNA is shown on

Journal Pre-proof

merge images. Histograms represent the relative pixel intensity of each protein in control and Ctail expressing cells. ***: p-values <0.001. Scale bar: 10 µm.
(B and D) Effect of Ctail expression on the duration of Lifeact-GFP (B) and 3xGFP-anillin (D) accumulation at apical cell-cell contacts. (B) Upper images show kymographs of orthogonal projections of one lateral plasma membrane at the division site of cells co-expressing lifeact-GFP alone (control) and Lifeact-GFP and Ctail (Ctail). Images are from the onset of fluorescent protein accumulation to the onset of ring constriction. a. : apical, b. : basal. Below, images are orthogonal projections of the plasma membrane at the division site of cells co-expressing Lifeact-GFP alone (control) and Lifeact-GFP with Ctail (Ctail) from the cytokinesis onset to the beginning of actomyosin ring constriction. (C) Histograms represent the time between the onset of proteins accumulation and actomyosin ring constriction for Lifeact-GFP alone (grey, n=11) and Lifeact-GFP and Ctail (brown, n=15). The p-value is indicated.
(D and E) Same as in B and C with 3xGFP-Anillin. n=17 and 11 for respectively 3xGFP-anillin alone and 3xGFP-anillin with Ctail.

Fig. 5. Depletion of α catenin increases the duration of ring formation.
(A) Endogenous α catenin and C-cadherin in embryos injected with α-catenin morpholino and RFP-membrane mRNA used as a tracer. For each condition, an image of a field containing cells expressing and not expressing RFP-membrane (asterisks) is shown. Red and blue bars on merged images indicate cell–cell contacts where fluorescence was quantified. Cells that do not express RFP-membrane are used as an internal control for fluorescence quantification. Line scans on the right show α-catenin and C-cadherin pixel intensity in internal control (blue) and cells expressing the RFP-membrane. Scale bars: 10 µm.
(B) Kymograph of a baso-lateral plasma membrane at the site of division of a cell expressing Lifeact-GFP in control or α catenin morpholino. Histogram is the time of Lifeact-GFP accumulation in control or α-catenin morpholino (n=12 and 24 for respectively control and α catenin morpholinos). The p-value is indicated.
(C) Same as in B with 3xGFP-Anillin instead of Lifeact-GFP. (n=9 and 19 for respectively control and α catenin morpholinos)
(D) Schematic representation of cytokinesis initiation in polarized epithelial cells. The mitotic furrow, which is asymmetrically positioned along the apicobasal axis, signals

the position of the contractile ring to the apical cell-cell contacts. This leads to extremely rapid ring formation spreading laterally from apical contacts towards the basal side of cells.

Journal Pre-proof

Journal Pre-proof

Supplementary figure legends

Fig. S1. (related to Fig. 1): MKLP1 and ECT2 were detected with specific antibodies in fixed embryos.
(A and C) Surface views and orthogonal projections of cells in interphase are shown for each protein. Arrowheads point to the concentration of the labelling at the apical junctions.
(B and D) Surface views and orthogonal projections of cells in anaphase are shown for each protein. Orthogonal projections along the equatorial axis (horizontal) and along the axis passing by the cell poles (vertical) are shown. Black arrowheads point to the concentration of the labelling at the apical and lateral junctions. Scale bars: 10 µm.

Fig. S2. (related to Fig. 2):
(A) The four fluorescent proteins Lifeact-GFP (a probe for F-actin), SF9-GFP (a probe for Myosin Heavy Chain), 3xGFP-anillin and GFP-Rock II KR localize at apical cell junctions in interphase cells. Representative surface views are presented. Below, orthogonal views are shown. White dotted lines on surface images symbolize the plan of orthogonal projection. Arrowheads indicate apical accumulation of fluorescent proteins.
(B) The duration of the actomyosin ring constriction is not significantly modified by expression of indicated fluorescent cytokinetic proteins compared with GFP-GPI.. The number of dividing cells analysed were 15, 16, 19, 17 and 17 for GFP-GPI, Lifeact-GFP, SF9-GFP, 3GFP-anillin and GFP-Rock II K/R, respectively. Statistical comparison between GFP-GPI and each fluorescent protein was made; p values are indicated on bars.
(C) Still images of a representative division of a cell expressing 3xGFP-anillin. Apical views are shown. Below, orthogonal projections through the plan parallel to the division site indicated by a dotted line. Times are indicated in seconds. Scale bars: 10 µm.

Fig. S3. (related to Fig. 2): Still images of cells expressing GFP-GPI alone (A) and ZO1-GFP co-expressed with RFP-GPI (B). In panel B, images corresponding to a confocal plane at the level of tight junctions marked by ZO-1, and a confocal plane 15

µm below tight junctions are presented. Time 0 corresponds to the onset of actomyosin ring constriction at the basal side. Below surface views, orthogonal projections through the axis indicated by dashed lines passing by the division site. Scale bars: 10 µm.

Fig. S4. (Related to Fig. 2): Apicobasal position of the mitotic spindle. Embryos were fixed and processed for indirect immunofluorescence to detect the mitotic spindle, cell-cell contacts and chromosomal DNA (red). Top images: confocal plane passing by the mitotic spindle poles. An orthogonal projection along the dashed line in top image is shown below. White arrows point on the spindle poles. The mean values for cell height and the distance of the mitotic spindle from apical and basal surfaces of cells are indicated (±SEM, n = 20 spindles in 2 embryos). Scale bar: 10 mm.

Fig. S5. (related to Fig. 3): (A) Still images of cells expressing the GFP-rGBD probe at a subapical confocal plane (Z0), 2 µm and 4,5 µm below. The upper panel show cells expressing high levels of GFP-rGBD (and consequently highly fluorescent) while the lower panel shows cells expressing lower levels of GFP-rGBD. Arrowheads point on GFP-rGBD localised at the cell equator when ring constriction is already advanced. GFP-rGBD enrichment at the cell equator is absent in early cytokinesis. These cells are representative of 16 analysed cells. (B) Validation of anti-phosphoS19MRLC antibodies. Embryos were fixed and treated with phosphatase buffer without (left) and with phosphatase (right). 3 confocal planes are presented. The orthogonal projections through the axis passing by the division site indicated by dashed lines on the front view are shown for each condition. Scale bars: 10 µm.

Fig. S6. (related to Fig. 4): Tight junctions are unaffected by Ctail. Embryos expressing RFP-gpi alone (control) and co-expressing Ctail with RFP-gpi (membrane) used as a tracer were fixed and processed for indirect immunofluorescence with antibodies against the tight junction proteins ZO-1 and occludin. Apical confocal planes and orthogonal projections are shown. DNA is shown on merge images. Histograms represent the relative pixel intensity of each proteins in control and Ctail expressing cells. n.s.: not signficant. Scale bars: 10 µm.

Fig. S7. (related to Fig. 5): Cells expressing 3xGFP-anillin in control or α-catenin and ZO-1 morpholinos. For each condition, still images of a representative dividing cell are shown. Apical views are shown. Below, orthogonal projections through the plan parallel to the division site indicated by a dotted line. Times are indicated in seconds. Scale bars: 10 µm.

Journal Pre-proof

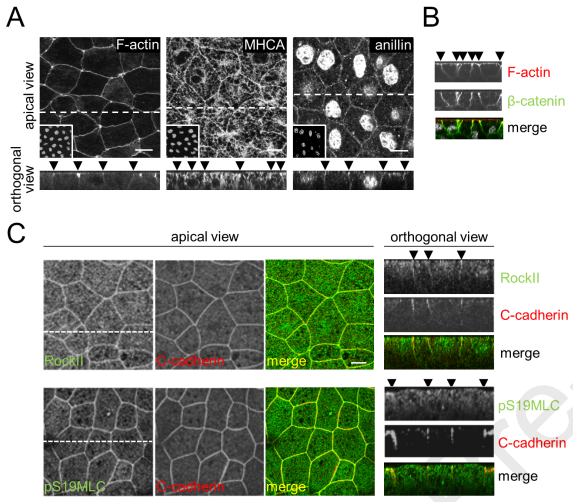


Figure 1

Journal Pre-proof

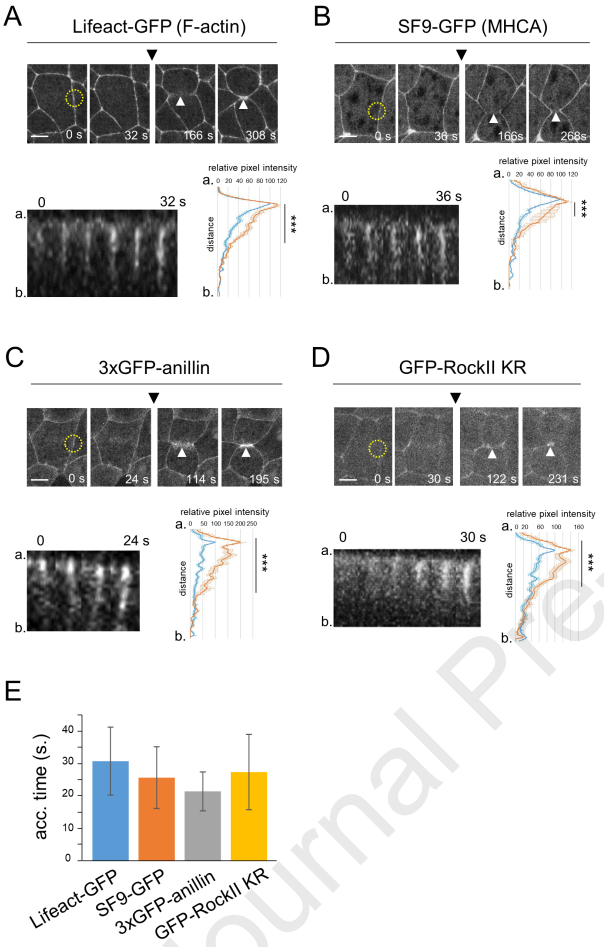


Figure 2

Journal Pre-proof

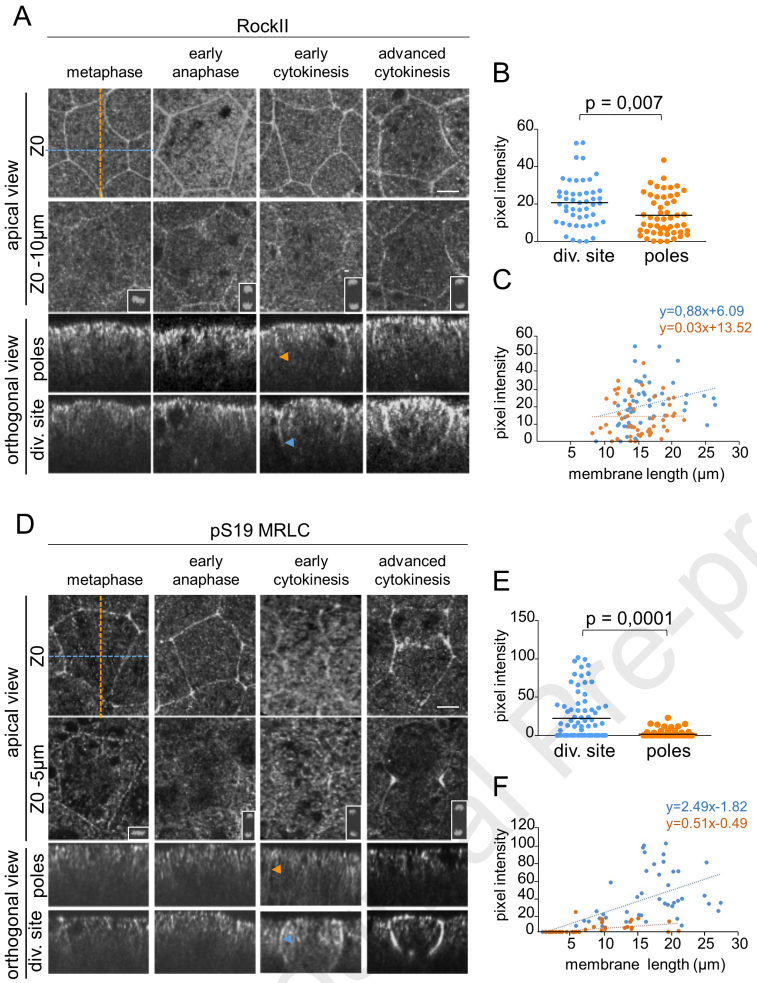


Figure 3

Journal Pre-proof

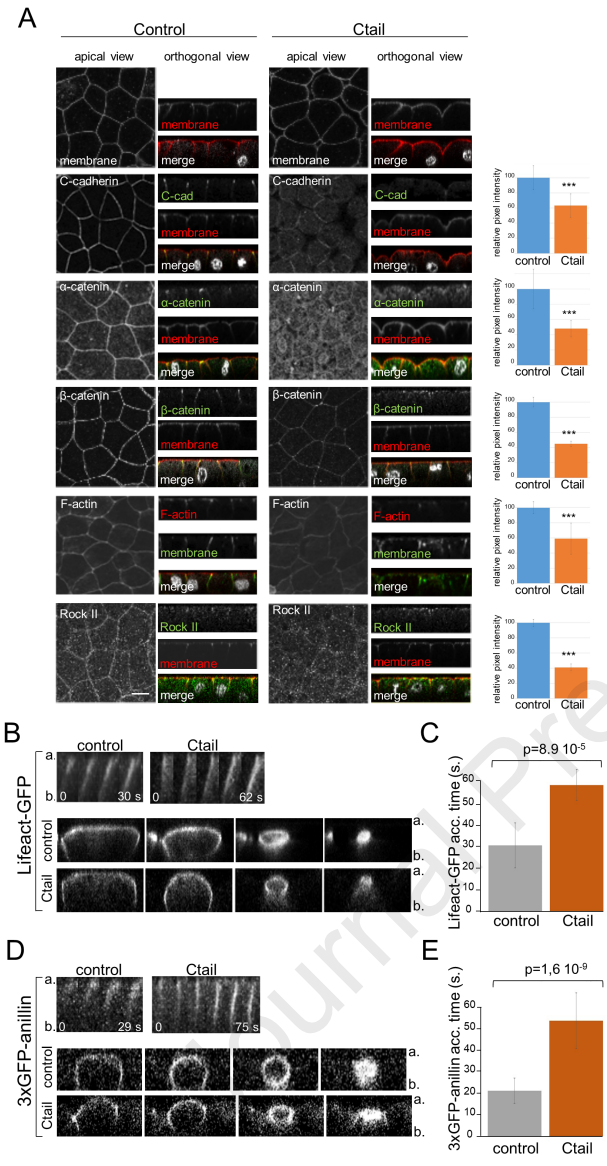


Figure 4

Journal Pre-proof

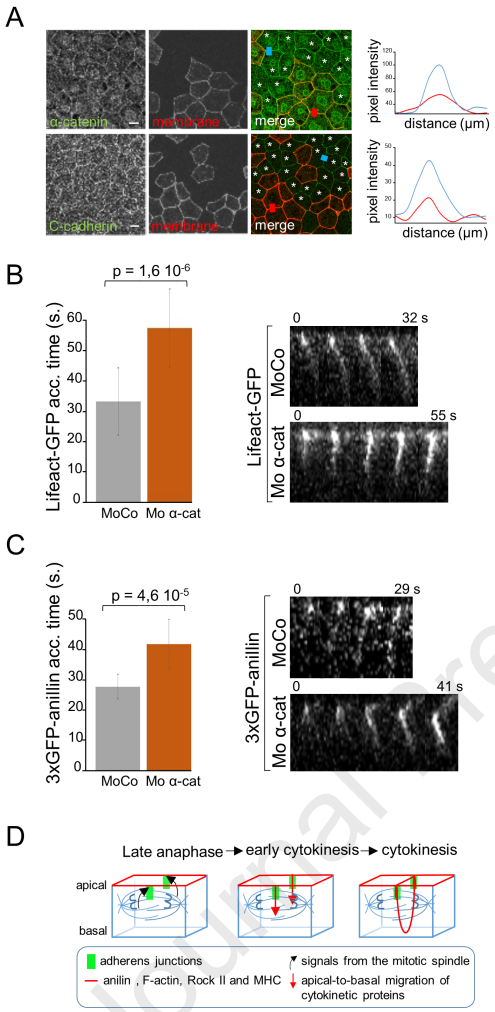


Figure 5

Journal Pre-proof

Journal Pre-proof

Highlights :

- The actomyosin contractile ring formation is polarised in epithelial cells
- Activation of the contractile ring is polarized in epithelial cells
- Adherens junctions are involved in the kinetics of the contractile ring formation
- Adherens junctions and the contractile ring are linked from the onset of cytokinesis
- High temporal resolution microscopy of epithelial cells in the *Xenopus* embryos

Journal Pre-proof

Conflict of interest

The authors declare no conflict of interest.

Journal Pre-proof